STUDY OF UNSTEADY TWO-DIMENSIONAL HORIZONTAL SEEPAGE FLOW USING THE FINITE ELEMENT METHOD

The Hung Nguyen¹, *Nguyen Hoang Phuong Luong ¹, Van Da Ho², Thi My Linh Nguyen¹, Ha Quoc Tin Nguyen³

¹Nam Can Tho University, Faculty of Architecture, Construction, and Environmental Studies, Can Tho City, Vietnam, ²People's Committee of Kon Tum Province, Vietnam, ³ Tay Do University, Can Tho City, Vietnam.

*Corresponding Author, Received: 18 June 2025, Revised: 16 July 2025, Accepted: 24 July 2025

ABSTRACT: The finite element method (FEM) based on the Galerkin approach is an effective technique for modeling groundwater flow and analyzing seepage, particularly in complex and heterogeneous geological environments. It allows for accurate simulation of groundwater levels, seepage velocity, and pore water pressure, supporting reliable predictions essential for water resource and geotechnical engineering. This study applies the Galerkin-based FEM to evaluate groundwater behavior in Kon Tum City, Vietnam. A computational program developed by the authors using the Fortran language was employed to simulate various groundwater extraction scenarios. Using field data, the model assessed the storage capacity, predicted changes in groundwater levels, and calculated seepage velocity under different pumping conditions. The method's ability to handle complex boundary conditions contributed to the precision of the simulations. The results demonstrate the FEM's effectiveness in groundwater modeling and its practical applicability in managing water resources and planning sustainable groundwater extraction strategies.

Keywords: Galerkin Finite Element Method, Two-Dimensional Horizontal Seepage Flow, Groundwater Extraction

1. INTRODUCTION

There are two methods in groundwater modeling and seepage analysis, namely the traditional experimental method and the numerical method. Traditional approaches in groundwater modeling and seepage analysis [1]. (i) Classical analytical methods to groundwater flow problems are based on Darcy's law and the continuity equation. These methods are well-suited for simple geometries and homogeneous, isotropic media. Although they yield exact solutions, their applicability is limited by simplifying assumptions such as homogeneity of the porous medium, steady-state or linearized flow conditions and geometrically regular boundaries. (ii) investigations Traditional field rely measurements of groundwater levels from observation wells and piezometers. However, they are generally unsuitable for heterogeneous or anisotropic conditions.

Numerical Methods in Groundwater Flow and Seepage modeling: (i) The finite difference method (FDM) is widely employed to simulate flow in both saturated and unsaturated porous media [2-4]. It solves the governing differential equations by discretizing them over a rectangular grid, making it suitable for modeling large-scale aquifer systems. However, FDM is limited in its ability to handle complex geometries and irregular boundaries, and it lacks flexibility in mesh refinement. (ii) The FEM has become a powerful tool in groundwater modeling due to its capacity to manage complex

domain geometries, represent heterogeneous and anisotropic conditions, and accommodate intricate boundary conditions [5]. The study of groundwater has been investigated by researchers using various methods [6-17].

The Galerkin FEM is particularly well-suited for complex seepage and groundwater flow problems due to its ability to implement adaptive meshing, thereby enhancing accuracy in critical zones such as seepage faces, drains, or impermeable barriers. It supports heterogeneous and anisotropic media through element-wise assignment of material properties. The method also offers high-order accuracy and the flexibility to handle irregular geometries—capabilities that are often limited in finite difference approaches. Galerkin FEM represents a robust and comprehensive modeling tool [18-24].

Surface water from rivers in Kon Tum City – Viet Nam is heavily impacted by overexploitation for agriculture, industry, and domestic use, combined with climate change causing prolonged droughts and reduced river flows. Groundwater serves as a sustainable alternative, providing a more stable water supply during dry seasons. However, groundwater extraction must be strictly managed to prevent depletion of aquifers, land subsidence...

Previous studies on groundwater reserves and exploitation potential in Kon Tum City have primarily relied on exploratory drilling methods, utilizing data from water pumping experiments conducted at boreholes. No scientific research on

this topic has yet employed modern numerical methods, such as the finite difference method or the finite element method. In this paper, we determine the storage capacity, changes in groundwater levels, and seepage velocity during groundwater extraction in Kon Tum City, Vietnam. The authors have developed a computational program based on the Galerkin FEM to solve the unsteady seepage equation. The model's computational results have predicted changes in groundwater levels and seepage velocity under various water resource exploitation scenarios.

2. RESEARCH SIGNIFICANCE

This study holds significant value in advancing the understanding and management of groundwater resources in Kon Tum City, Vietnam. By applying the Galerkin FEM to model two-dimensional unsteady horizontal seepage flow, the research provides a robust computational framework for predicting groundwater level fluctuations and seepage velocities under various extraction scenarios. This approach overcomes the limitations of traditional analytical and field-based methods, offering a more precise and flexible tool for geotechnical engineering and water resource management. The findings contribute critical insights into sustainable groundwater exploitation and provide a scientific foundation for urban planning and resource management in water-scarce regions of Vietnam.

3. THEORY OF COMPUTATION

The seepage flow in soil is calculated based on the seepage equation, which is established using Darcy's law and the continuity equation for seepage flow. In conditions where the geological distribution with depth varies little, the two-dimensional horizontal (2DH) seepage equation can be applied for calculations.

3.1. The Equation of Unsteady Two-Dimensional **Horizontal Flow:**

The equation of unsteady two-dimensional $\frac{\partial}{\partial x} \left(K_x \frac{\partial h}{\partial x} \right) + \frac{\partial}{\partial y} \left(K_y \frac{\partial h}{\partial y} \right) + q = S_s \frac{\partial h}{\partial t}$

Where S_s : the storativity (dimensionless); t: time (sec); h: Hydraulic head (m); K: Hydraulic conductivity (m/s), typically assumed to be constant in the medium; x,y: spatial coordinates in the horizontal plane; q: Flow rate at the source point; q has a negative value (-) if the flow is extracted from the domain and (+) if the flow is added to the domain.

3.2. Discretization in Space

In space, the Galerkin finite element method is applied; the interpolation function is chosen as

$$h^{(e)} = \sum_{i=1}^{n} N_i h_i \tag{2}$$

 $h^{(e)}$: The approximate value of the hydraulic head in element $A^{(e)}$; N_i : The shape function at node i in element $A^{(e)}$; n: The number of nodes in element $A^{(e)}$; h_i : The unknown value of the hydraulic head at node *i* of element $A^{(e)}$.

Applying the Galerkin finite element method established in weak form, using integration by parts with second-order derivatives; assuming that at each element $A^{(e)}$, the permeability coefficients in the x and y directions remain constant, we have:

and
$$y$$
 directions remain constant, we hat
$$R_i^{(e)} = -\iint_{A^{(e)}} N_i^{(e)} \left[K_x^{(e)} \frac{\partial^2 \hat{h}^{(e)}}{\partial x^2} + K_y^{(e)} \frac{\partial^2 \hat{h}^{(e)}}{\partial y^2} + q^{(e)} - S_s^{(e)} \frac{\partial \hat{h}^{(e)}}{\partial t} \right]$$

$$dxdy = 0$$
(3)
$$-\iint_{A^{(e)}} N_i^{(e)} \left[K_x^{(e)} \frac{\partial^2 \hat{h}^{(e)}}{\partial x^2} + K_y^{(e)} \frac{\partial^2 \hat{h}^{(e)}}{\partial y^2} + q^{(e)} \right] dxdy$$

$$+\iint_{A^{(e)}} N_i^{(e)} S_s^{(e)} \frac{\partial^2 \hat{h}^{(e)}}{\partial t} dxdy = 0$$

Integration by parts (Green's formula). Consider the boundary segment $d\Gamma$ of a curve enclosing a twodimensional region $\Omega = A^{(e)}$, in the case of a closed curve, we have:

$$\begin{split} & \int\!\int_{\Omega}\!\phi\frac{\partial\psi}{\partial x}\,dxdy \equiv -\!\int\!\int_{\Omega}\!\frac{\partial\phi}{\partial x}\psi\,dxdy + \oint_{\Gamma}\!\phi\psi\,n_{x}d\Gamma \\ & \int\!\int_{\Omega}\!\phi\frac{\partial\psi}{\partial y}\,dxdy \equiv -\!\int\!\int_{\Omega}\!\frac{\partial\phi}{\partial y}\psi\,dxdy + \oint_{\Gamma}\!\phi\psi\,n_{y}d\Gamma \end{split}$$

Substituting into equation 3, we obtain equation 4.
$$\iint_{A^{(e)}} N_i^{(e)} \left[K_x^{(e)} \frac{\partial N_i^{(e)}}{\partial x} \cdot \frac{\partial \hat{h}^{(e)}}{\partial x} + K_y^{(e)} \frac{\partial N_i^{(e)}}{\partial y} \cdot \frac{\partial \hat{h}^{(e)}}{\partial y} \right] dx dy$$

$$+ \iint_{A^{(e)}} N_i^{(e)} S_s^{(e)} \frac{\partial \hat{h}^{(e)}}{\partial t} dx dy$$

$$- \int_{C^{(e)}} N_i^{(e)} \left(K_x^{(e)} \frac{\partial \hat{h}^{(e)}}{\partial x} l + K_y^{(e)} \frac{\partial \hat{h}^{(e)}}{\partial y} m \right) ds - F_i^{(e)} = 0$$
 (4)

l, m: Cosines of the direction of the outward normal vector at the boundary; $K_{x}^{(e)}$ $K_{y}^{(e)}$: Permeability coefficients in the x and y directions, respectively, of element $A^{(e)}$; $A^{(e)}$: Area of element e. Based on the above results, we define the algebraic sum of the first two terms of equation 4 as:

$$\begin{bmatrix}
R_{1}^{(e)} \\
R_{2}^{(e)} \\
\vdots \\
R_{n}^{(e)}
\end{bmatrix} = \begin{bmatrix}
K^{(e)} \\
h_{2} \\
\vdots \\
h_{n}
\end{bmatrix} - \begin{bmatrix}
F_{1}^{(e)} \\
F_{2}^{(e)} \\
\vdots \\
F_{n}^{(e)}
\end{bmatrix} - \begin{bmatrix}
G_{1}^{(e)} \\
G_{2}^{(e)} \\
\vdots \\
G_{n}^{(e)}
\end{bmatrix} (5)$$

The third term is determined as follows:

$$\iint_{A^{(e)}} N_i^{(e)} S_s^{(e)} \frac{\partial \hat{h}^{(e)}}{\partial t} dx dy = \iint_{A^{(e)}} N_i^{(e)} S_s^{(e)} \left[N_1^{(e)} \dots N_n^{(e)} \right] \left\{ \begin{array}{l} \frac{\partial h_1}{\partial t} \\ \frac{\partial h_2}{\partial t} \\ \vdots \\ \frac{\partial h_n}{\partial t} \end{array} \right\} (6)$$

It can be rewritten in matrix form as follows:

$$\begin{bmatrix}
R_{1}^{(e)} \\
R_{2}^{(e)} \\
\vdots \\
R_{n}^{(e)}
\end{bmatrix}_{C} = \begin{bmatrix}
C^{(e)} \\
\vdots \\
\frac{\partial h_{1}}{\partial t} \\
\frac{\partial h_{2}}{\partial t} \\
\vdots \\
\frac{\partial h_{n}}{\partial t}
\end{bmatrix}$$
(7)

 $\lceil C^{(e)} \rceil$: capacity element matrix, with:

$$\left[C^{(e)}\right] = \iint\limits_{A^{(e)}} \begin{bmatrix} N_1^{(e)} \\ \vdots \\ N_n^{(e)} \end{bmatrix} \left[S_S^{(e)}\right] \left[N_1^{(e)}....N_n^{(e)}\right] dxdy$$
 (8)

In this paper, we use the lumped element formulation to calculate $[C^{(e)}]$. For a triangular element with three vertices at nodes i, j, and k, we obtain the following

$$N_i^{(e)} N_j^{(e)} = \begin{cases} \frac{1}{3} & \text{if } i = j \\ 0 & \text{if } i \neq j \end{cases}$$

$$\tag{9}$$

We have:

$$\left[C^{(e)} \right] = \frac{S_S^{(e)} A^{(e)}}{3} \begin{bmatrix} 1 & 0 & 0 \\ 0 & 1 & 0 \\ 0 & 0 & 1 \end{bmatrix}$$
(10)

3.3. The Element Matrix Equation:

$$\lceil KK \rceil \{qq\} = \{BB\} \tag{11}$$

Where:
$$\{qq\} = (h_1^{n+1}, h_2^{n+1}, h_3^{n+1})^T$$
 (12)

 h_i^{n+1} The hydraulic head height at node i at time step n+1. $\lceil KK \rceil$ The element stiffness matrix of size 3x3. $\{BB\}$: A vector with 3 components:

$$\{BB\} = (BB_1, BB_2, BB_3)^T$$
 (13)

3.4. Discretization in time Using Weighted Finite **Difference**

For the entire computational domain, we have the overall capacitance matrix with p nodes and melements:

$$[C] = \sum_{i=1}^{m} [C^{(e)}] \tag{14}$$

Assembling the equations written for all elements of the entire computational domain, we obtain:

$$\begin{bmatrix} C \end{bmatrix} \left\{ \begin{array}{c} \frac{\partial h_1}{\partial t} \\ \vdots \\ \frac{\partial h_p}{\partial t} \end{array} \right\} + \begin{bmatrix} K \\ \vdots \\ h_p \end{bmatrix} = \{F\} + \{G\}$$

$$(15)$$

The two vectors $\{h^*\}$ and $\{h\}$ are defined as follows:

$$\left\{h^*\right\} = \begin{cases} \frac{\partial h_1}{\partial t} \\ \vdots \\ \frac{\partial h_p}{\partial t} \end{cases}, \quad \left\{h\right\} = \begin{cases} h_1 \\ \vdots \\ h_p \end{cases}$$

$$(16)$$

Equation 15 can be rewritten as:

$$\lceil C \rceil \{h^*\} + \lceil K \rceil \{h\} = \{F\} + \{G\}$$
 (17)

Applying time difference:

$$\frac{\partial h}{\partial t} \cong \frac{h(t + \Delta t) - h(t)}{\Delta t} \tag{18}$$

$$\frac{\partial h}{\partial t} \approx \frac{h(t + \Delta t) - h(t)}{\Delta t}$$

$$h(\varepsilon) \approx h(t) + (\varepsilon - t) \frac{\partial h}{\partial t} = h(t) + (\varepsilon - t) \frac{h(t + \Delta t) - h(t)}{\Delta t} s$$
 (19)

The variable ε is defined as follows

$$\omega = \frac{(\varepsilon - t)}{\Delta t} \tag{20}$$

Where: ω is the time weight

We have reversed the positions of equations 19 and 20 to be more logical

$$h(\varepsilon) = (1 - \omega)h(t) + \omega h(t + \Delta t) \tag{21}$$

Extension for vectors h, F, G:

$$\{h\} = (1 - \omega)\{h\} + \omega\{h\}_{+++}$$
 (22)

$$\{F\} = (1 - \omega)\{F\}_t + \omega\{F\}_{t+\Delta t}$$
 (23)

$$\{G\} = (1 - \omega)\{G\}_t + \omega\{G\}_{t + \Delta t}$$
 (24)

Substitute the above formulas into equation 17 we

$$([C] + \omega \Delta t [K]) \{h\}_{t+\Delta t} =$$

$$([C] - (1 - \omega) \Delta t [K]) \{h\}_{t} +$$
(25)

$$\Delta t \Big((1 - \omega) \big\{ F \big\}_t + \omega \big\{ F \big\}_{t + \Delta t} \Big) +$$

$$\Delta t \Big((1-\omega) \Big\{ G \Big\}_t + \omega \Big\{ G \Big\}_{t+\Delta t} \Big)$$

The value of $\{h\}$ at the initial time $t = t_0$ is: $\{h\}_{t}$

prescribed value. Using equation 25 to solve for the value of $\{h\}$ at the end of the first time step $\{h\}_{to+\Delta t}$. Then, set: $\{h\}_t = \{h\}_{to+\Delta t}$. This process is repeated for subsequent time steps. Depending on the choice of the value ω , we have: Choosing $\omega = 0$ (forward difference), equation becomes: $[C]{h}_{t+\Delta t} = ([C] - \Delta t[K]){h}_{t}$ $+\Delta t \{F\}_{t} + \Delta t \{G\}_{t}$

Choosing $\omega = \frac{1}{2}$ (central difference), equation 25 becomes:

$$\left(\begin{bmatrix} C \end{bmatrix} + \frac{\Delta t}{2} \begin{bmatrix} K \end{bmatrix} \right) \left\{ h \right\}_{t+\Delta t} = \left(\begin{bmatrix} C \end{bmatrix} - \frac{\Delta t}{2} \begin{bmatrix} K \end{bmatrix} \right) \left\{ h \right\}_{t}$$

$$+ \frac{\Delta t}{2} \left(\left\{ F \right\}_{t} + \left\{ F \right\}_{t+\Delta t} \right) + \frac{\Delta t}{2} \left(\left\{ G \right\}_{t} + \left\{ G \right\}_{t+\Delta t} \right)$$

Choosing $\omega = 1$ (backward difference), equation

25 gives us:

$$([C] + \Delta t[K]) \{h\}_{t+\Delta t} = [C] \{h\}_{t} + \Delta t \{F\}_{t+\Delta t}$$

$$+ \Delta t \{G\}_{t+\Delta t}$$

3.5. Pairing the Elements

Assume we are considering a seepage problem with pressure in a domain Ω , where the domain is divided into multiple triangular elements. At each node, there are s degrees of freedom (number of unknowns at the node). Here, s=1 represents the seepage water column. Each triangular element has 3 nodes (r=3), so the number of degrees of freedom for each element is $r \times s = 3 \times 1 = 3$. Each triangular element is numbered at its nodes (i, j, k) in a conventional direction (counterclockwise), with node i conventionally defined as the leftmost and lowest node (see Fig 1). For any arbitrary element n_e , we have the element matrix $[K]_e$ as follows:

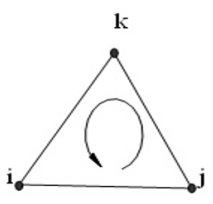


Fig 1. Node numbering convention and element matrix

$$[K]_{e} = \begin{bmatrix} K_{ii}^{e} & K_{ij}^{e} & K_{ik}^{e} \\ K_{ji}^{e} & K_{jj}^{e} & K_{jk}^{e} \\ K_{ki}^{e} & K_{kj}^{e} & K_{kk}^{e} \end{bmatrix}$$

Global matrix:

$$[K] = \sum_{1}^{n} [K]_{e}$$

Similarly for the global matrices of other element matrices. In the global matrix, the non-zero elements do not have a diagonal form (also known as a banded form). To save memory and computational time, only the non-zero elements are stored, and the algorithm only performs calculations with these non-zero elements.

3.6. Global Matrix Equation

$$|K|\{q\} = \{B\} \tag{29}$$

Where: [K] The global matrix; $\{q\}$ The global unknown vector.

3.7. Assigning Boundary Conditions

After obtaining the system matrix in banded form, to simplify programming, the size of the global matrix for the problem is fixed regardless of the number of boundary conditions. The equation takes

the form:
$$[K].\{q\} = \{B\}$$
 (30)

If the i = r unknown is known to be α_i , it means $q_r = \alpha_i$, then the coefficients of the system matrix are modified as follows:

$$K_{rj} = 0$$
 if $j \neq r$
 $K_{ir} = 0$ if $i \neq r$
 $K_{rr} = 1$ (31)

The right-hand side vector of the system will be:

Then eliminate row r and column r from the system of matrix equations.

3.8. Linear Algebraic Equations

The system of linear algebraic equations has the form :

$$\left\{ \overrightarrow{K}^{*}\right\} \left\{ \overrightarrow{q}^{*}\right\} = \left\{ \overrightarrow{B}^{*}\right\} \tag{33}$$

Equation 33 is in matrix form; which solution we choose depends on the type of problem, the properties of the storage matrix, and the way the overall matrix is stored. It can be solved by Gauss, Seidel, Cholesky elimination methods... In this paper, we choose the Cholesky solution because it is simple, computationally efficient, saves memory, and has good numerical stability.

3.9. Programming in Fortran

To solve the seepage problem, the program is written according to the block diagram (see Fig 2).

The algorithm and computational program have been validated for assessing the extent of saltwater intrusion from the East Sea into the Bau Tro reservoir, Quang Binh Province, Vietnam, under conditions of freshwater extraction during the dry season [25].

4. APPLYING CALCULATIONS TO THE STUDY AREA.

4.1. Introduction to the Study Area

Kon Tum City is located in the North Central Highlands, currently the water source for the city is mainly surface water taken from the Dak Bla River. Urban development in recent years has led to a rapid increase in water demand. Therefore, in addition to using surface water taken from rivers in the region, it is necessary to study groundwater. For Kon Tum City in the long-term development strategy, groundwater is still the best water source for drinking, daily life and other activities.

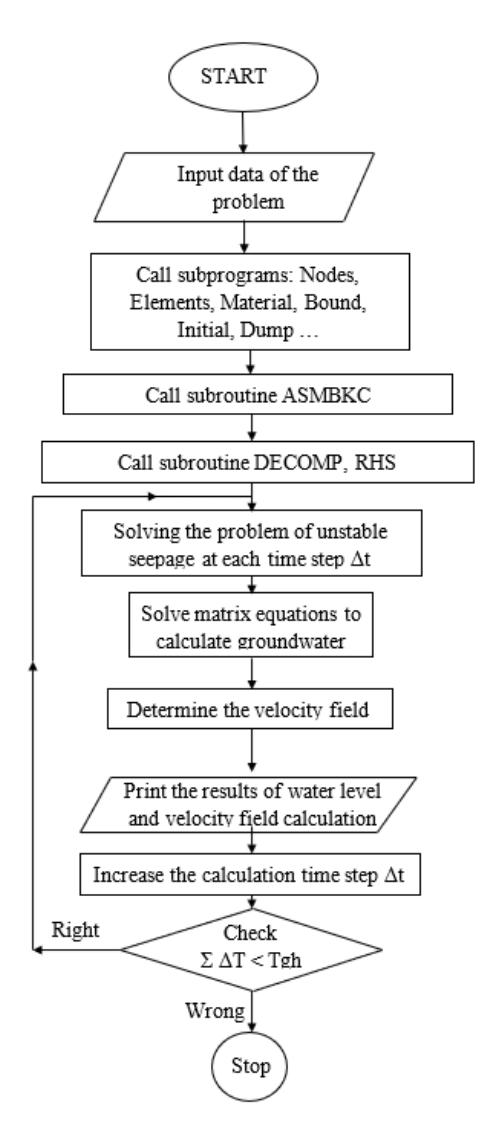


Fig 2. Algorithm diagram of seepage problem using finite element method.

Based on the synthesized hydrogeological survey data, it has been identified that the Kon Tum City area contains two principal aquifers: the Pleistocene aquifer (Qp) and the Neogene aquifer (m4). In general, the groundwater quality in both aquifers meets the permissible standards for basic domestic use. The Neogene aquifer is widely distributed, covering nearly the entire study area with an estimated surface area of approximately 122 km². In contrast, the Pleistocene aquifer is more limited in extent, primarily located in the central part of the city, with a surface area of around 20 km². According

to research conducted by the Department of Science and Technology of Kon Tum City, the hydrogeological parameters of the region are presented in Table 1. The exploitable groundwater reserves at boreholes, estimated using simplified analytical formulas, are shown in Tables 2 [26].

Table 1. Hydrogeological parameters of Kon Tum City

No.	Boreholes	Pump flow (m/day)	K (m/day)	K _H , K _m (m ² /day)	μ, μ*
1	BH TD4	527,9	1,42	68,18	0,138
2	BH DK1	623,0	5,05	232,3	0,263
3	BH T.Doi	259,2	3,0	48,6	0,203
4	BH 160	363,6	2,66	106,4	0,191
5	BH 158	522,5	5,31	84,96	0,27
6	BH 154	394,6	3,78	68,04	0,227

K: Permeability coefficient; K_H , K_m : hydraulic conductivity; μ , μ^* : coefficient of water release

Table 2. Water reserves exploited at boreholes

No.	Boreholes	S (m)	Q (m³/day)	S _{kt} (m)	Qkt (m³/day)
1	BH T.Doi	8,6	259,2	19,3	582
2	BH TD4	9,0	527,9	19,8	1160
3	BH 160	4,01	363,6	8,8	798
4	BH 154	12,34	394,6	27,0	863

4.2. Computational Domain

Based on the hydrogeological map of the Kon Tum city area, the calculation zone is delineated. The GMS model is used to automatically generate a two-dimensional horizontal (2D) mesh. The computational domain and coordinate system (see Fig 3).

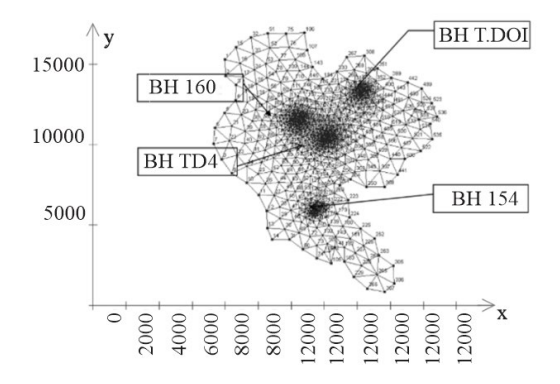


Fig 3. Computational domain and finite element mesh

Permeability coefficient of the aquifer in the calculated domain: $K_x = K_y = 2.67 \text{m/day}$. The storativity $S_s = 0.185$

4.3. Boundary Conditions and Initial Conditions

+ Initial condition: At time t = 0, the average groundwater level elevation is taken across the entire

domain H = 515(m)

+ Water level boundary condition: Based on the static water levels in the boreholes, the groundwater level elevation (relative to sea level) along the boundary of the calculation domain is calculated and interpolated, with values provided in Table 3.

Table 3. Head boundary condition at the nodes

1 531 514.5 14 350 2 399 514.5 15 304 3 442 514.5 16 261 4 489 514.5 17 223	H(m)
3 442 514.5 16 261 4 489 514.5 17 223	513.45
4 489 514.5 17 223	513.45
	513.45
	513.45
5 523 514.5 18 183	526.2
6 536 514.5 19 141	526.2
7 538 514.5 20 105	526.2
8 540 514.5 21 74	526.2
9 535 513.45 22 7	515
10 522 513.45 23 6	515
11 488 513.45 24 5	515
12 441 513.45 25 4	515
13 398 513.45	

- + On the remaining boundaries the inflow is zero (Q = 0).
- + In the area there are 04 experimental pumping boreholes with the following pumping flow rates:
- BH T.Doi: $Q = 259,2m^3/day$, node : 500, coordinate (16053.0, 13222.0)
- BH 160: $Q = 363,6m^3/day$, node : 375, coordinate (12207.0, 11433.0)
- BH TD4: $Q = 527.9 \text{ m}^3/\text{day}$, node : 515, coordinate (13924.0, 10199.0)
- BH 154: $Q = 394.6 \text{ m}^3/\text{day}$, node : 217, coordinate (13334.0, 5727.0)
 - + Calculation time T = 100 days
 - + Calculation time step dt = 1 day

4.4. Results

From the established program, we proceed to enter input data corresponding to the given boundary conditions and initial conditions. From the calculation results, we draw the water level and seepage velocity contours (Fig $4 \div 15$).

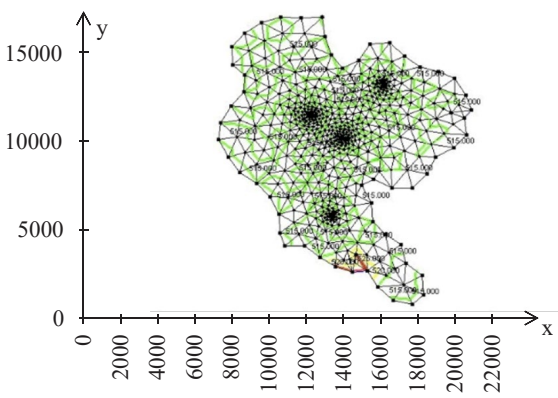


Fig 4. Groundwater level contour, experimental pumping flow, T = 15 days

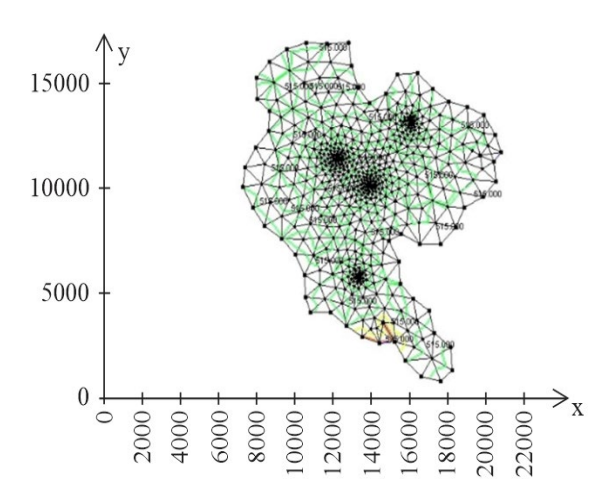


Fig 5. Groundwater level contour, experimental pumping flow, T = 50 days

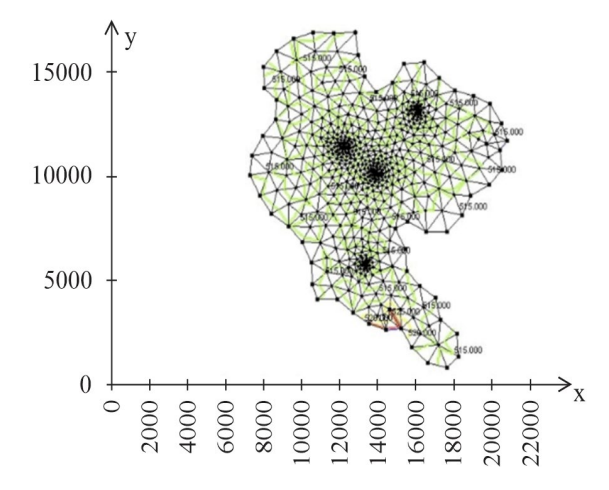


Fig 6. Groundwater level contour, experimental pumping flow, T = 100 days

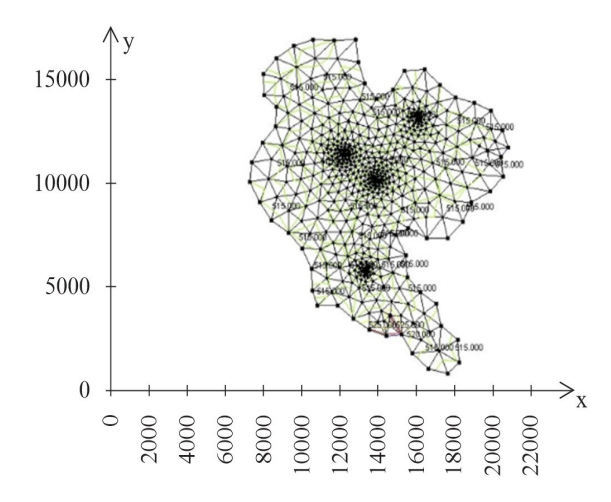


Fig 7. Groundwater level contour, the pumping flow rate, T = 100 days.

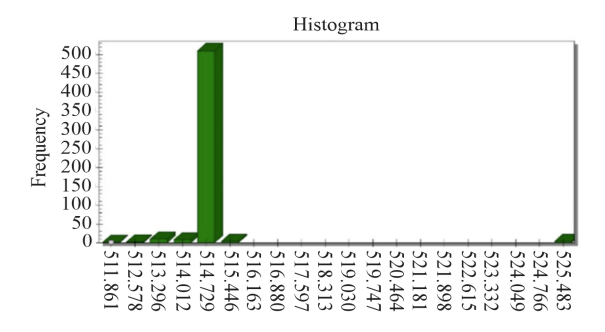


Fig 8. Statistical chart of groundwater level occurrence frequency, experimental pumping flow, T = 15 days

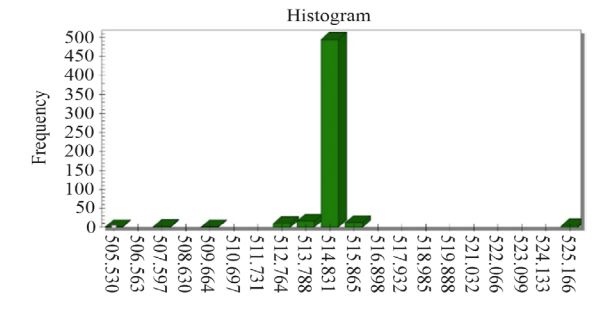


Fig 9. Statistical chart of groundwater level occurrence frequency, experimental pumping flow, T = 50 days

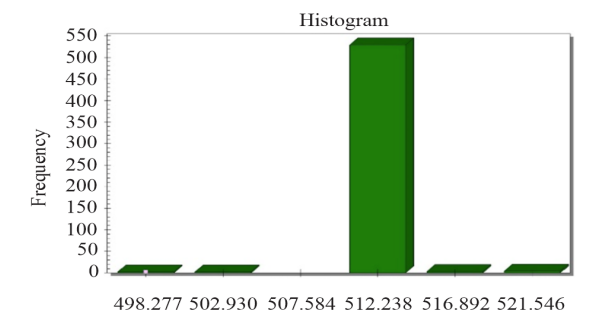


Fig 10. Statistical chart of groundwater level occurrence frequency, experimental pumping flow, T = 100 days

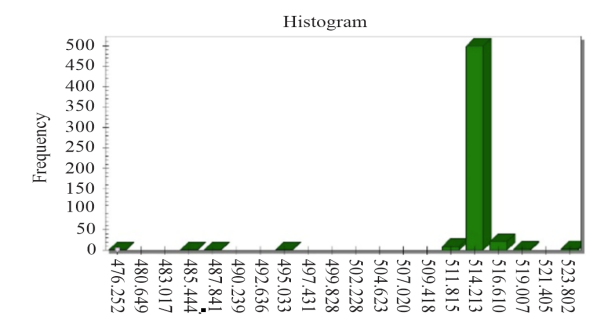


Fig 11. Statistical chart of groundwater level occurrence frequency, pumping flow rate, T = 100 days

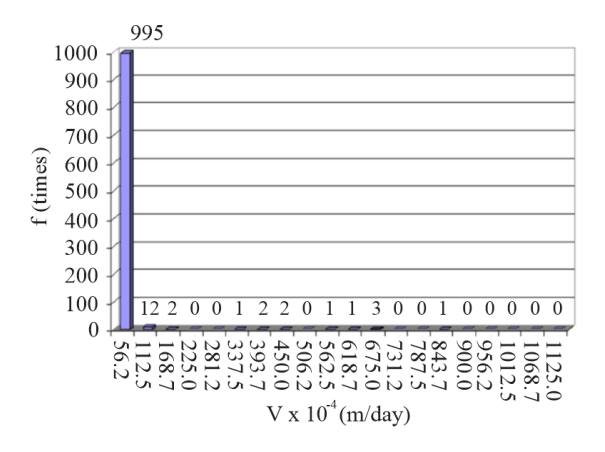


Fig 12. Statistical chart of seepage velocity, experimental pumping flow, T = 15 days

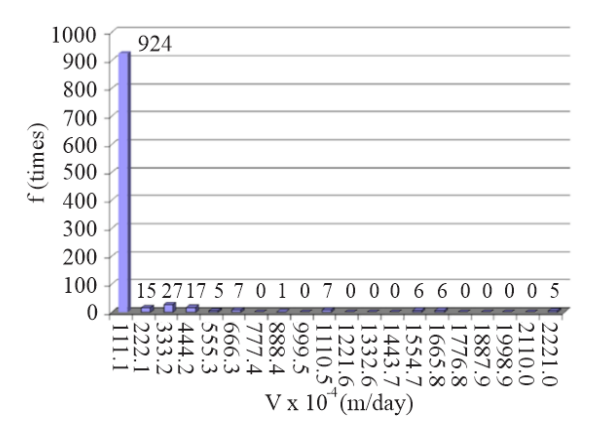


Fig 13. Statistical chart of seepage velocity, experimental pumping flow, T = 50 days

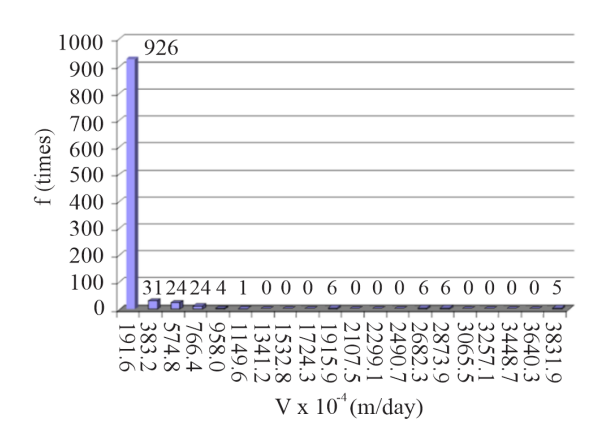


Fig 14. Statistical chart of seepage velocity, experimental pumping flow, T = 100 days

Based on the graph plotted from the calculation results, it is observed that the closer to the boreholes, the lower the groundwater level. For example, at borehole TD4, corresponding to a calculation period of 100 days, the radius of influence R=135m and the drawdown S=17m.

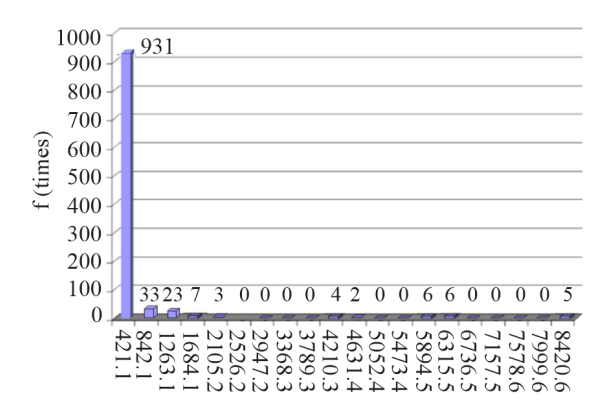


Fig 15. Statistical chart of seepage velocity, pumping flow rate, T = 100 days

Table 4. Results of calculating groundwater level in the calculation domain, pumping test; T= 100 days

Node	H(m)	Node	H(m)	Node	H(m)
1	515.01	10	515.00	19	515.01
2	514.99	11	515.00	20	515.00
3	515.00	12	515.01	21	514.99
4	515.00	13	515.00	22	515.00
5	515.00	14	515.01	23	514.97
6	515.00	15	514.99	24	514.97
7	515.00	16	515.00	25	515.01
8	515.01	17	515.01	26	514.99
9	515.02	18	515.00	27	515.00

Table 5. Results of calculating seepage velocity in the calculation domain, pumping test; T = 100 days

Node	$V_{\rm X}$	$V_{\rm Y}$	Node	V_x	V_y
1	3,023E-05	3,393E-05	10	3,585E-06	-1,72E-05
2	1,354E-05	-3,53E-05	11	1,625E-05	-1,03E-05
3	-3,621E-05	2,007E-05	12	1,459E-05	5,107E-06
4	-3,739E-05	-1,11E-05	13	9,169E-06	-9,28E-07
5	-1,496E-05	-2,84E-05	14	5,443E-06	1,920E-05
6	1,521E-06	2,364E-06	15	1,247E-04	-2,78E-05
7	-2,557E-05	2,968E-05	16	8,949E-05	1,013E-04
8	-3,473E-05	-1,85E-05	17	8,108E-05	1,035E-04
9	5,069E-06	-4,24E-06	18	9,809E-05	7,002E-05

The computational results from the model are crucial for establishing the foundation for the placement of pumps for groundwater extraction in the future. These results serve as one of the bases for determining land subsidence as well as the potential for subsurface erosion during water pumping. Additionally, the lowering of the groundwater level negatively impacts the groundwater exploitation of existing nearby structures and gives rise to several other issues, such as the growth and development of industrial crops.

4.5 Comments

From the results calculated by the mathematical model, the following basic parameters are obtained:

- + With the experimental pumping flow rate: The groundwater level at the boreholes fluctuates from $H_{\text{min}}=498~\text{m}$ to $H_{\text{max}}=513.5~\text{m},$ with a maximum seepage velocity $V_{\text{max}}=0.383~\text{m/day}.$
- + With the extraction pumping flow rate (Table 2): The groundwater level fluctuates from $H_{min} = 478$ m to $H_{max} = 511.5$ m, with a maximum seepage velocity Vmax = 0.842 m/day.

Based on the results obtained from the aforementioned mathematical model, it can be concluded that the groundwater resources in Kon Tum City are sufficient to meet the exploitable reserve demands. The model also provides predictions of groundwater level fluctuations within the urban area, serving as a foundational basis for the rational design and planning of groundwater extraction facilities.

5. CONCLUSION:

This study has developed an algorithm and program to solve the two-dimensional horizontal seepage equation. In the spatial direction, the equation is discretized using the Galerkin finite element method; in the time direction, it is discretized using the weighted difference method; the computational mesh is divided into triangular elements.

Based on the calculation results of the exploitable reserves for the Kon Tum city area; the exploitable reserves for structures and piezometric heads, and the seepage velocity with different planned extraction well configurations in the city area, the study concludes: With the future water demand for domestic use and other purposes in Kon Tum city potentially reaching 20.000 m³/day, the calculated exploitable reserves in the area are sufficient to meet the demand. However, appropriate extraction measures are necessary to ensure the long-term sustainability of the groundwater resources.

The fluctuation of groundwater levels combined with a relatively high seepage velocity may cause subsidence and underground erosion, affecting the quality of extraction and utilization of construction projects in the area. At the location where fluid flows from the wellbore, the significant pressure gradient differential may lead to potential erosion. Therefore, it is recommended to implement reverse filtration layers to mitigate erosion.

This procedure was applied and validated for the case of the Bau Tro reservoir in Quang Binh province, Vietnam [25]. The results confirm the suitability of the computational program developed by the research team.

6. ACKNOWLEDGEMENTS

The authors sincerely thank the Department of Science and Technology of Kon Tum City for providing documents and previous research results. Financial support from Nam Can Tho University, Vietnam, is also gratefully acknowledged. Additionally, we express our gratitude to the anonymous reviewers for their invaluable feedback, which greatly improved the manuscript.

7. REFERENCES

- [1] Pinder G.F. and Gray W.G, Finite Element Simulation in Surface and Subsurface Hydrology. Elsevier, 2013.
- [2] Anderson M.P, Woessner W.W, and Hunt R.J, Applied Groundwater Modeling: Simulation of Flow and Advective Transport, Second edition. London; San Diego, CA: Academic Press, 2015.
- [3] Ma R, "Modeling Groundwater Flow and Contaminant Transport," Vadose Zone Journal, vol. 10, p. 769, May 2011, doi: 10.2136/vzj2010.0151.
- [4] Sugimoto S. and Ishizuka Y, "Slope Deformation Monitoring using Wireless Sensor Network and Evaluation of Mechanical Stability by FDM Simulation," GEOMATE Journal, vol. 22, no. 94, Art. no. 94, June 2022.
- [5] Narasimhan T.N. and Witherspoon P.A, "Overview of the Finite Element Method in Groundwater Hydrology," in Finite Elements in Water Resources, K. P. Holz, U. Meissner, W. Zielke, C. A. Brebbia, G. Pinder, and W. Gray, Eds., Berlin, Heidelberg: Springer, 1982, pp. 29–44. doi: 10.1007/978-3-662-02348-8 2.
- [6] Karatzas G.P, "Developments on Modeling of Groundwater Flow and Contaminant Transport," Water Resour Manage, vol. 31, no. 10, pp. 3235– 3244, Aug. 2017, doi: 10.1007/s11269-017-1729-z.
- [7] Scudeler C, Paniconi C, Pasetto D, and Putti M, "Examination of the Seepage Face Boundary Condition in Subsurface and Coupled Surface/Subsurface Hydrological Models," Water Resources Research, vol. 53, no. 3, pp. 1799–1819, 2017, doi: 10.1002/2016WR019277.
- [8] Sikdar P.K, "Numerical Groundwater Modeling," in Groundwater Development and Management: Issues and Challenges in South Asia, P. K. Sikdar, Ed., Cham: Springer International Publishing, 2019, pp. 191–207. doi: 10.1007/978-3-319-75115-3 7.
- [9] Karamouz M, Ahmadi A, and Akhbari M, Groundwater Hydrology: Engineering, Planning, and Management, 2nd ed. Boca Raton: CRC Press, 2020. doi: 10.1201/9780429265693.
- [10]Říha J, "Groundwater Flow Problems and Their

- Modelling," in Assessment and Protection of Water Resources in the Czech Republic, M. Zelenakova, J. Fialová, and A. M. Negm, Eds., Cham: Springer International Publishing, 2020, pp. 175–199. doi: 10.1007/978-3-030-18363-9 8.
- [11]Ke X, Wang W, Xu X, Li J, and Hu H, "A Saturated–Unsaturated Coupling Model for Groundwater Flowing into Seepage Wells: a Modeling Study for Groundwater Development in River Basins," Environ Earth Sci, vol. 80, no. 21, p. 711, Oct. 2021, doi: 10.1007/s12665-021-10035-8.
- [12]Intui S, Jindawutthiphan J, Inazumi S, "Evaluation of Displacement on Unsaturated Soils in Bangkok Plain," GEOMATE Journal, vol. 23, no. 100, Art. no. 100, Dec. 2022.
- [13]Bakker M. and Post V, Analytical Groundwater Modeling: Theory and Applications using Python. London: CRC Press, 2022. doi: 10.1201/9781315206134.
- [14]El Rawy M, Zijl W, Salem A, Awad A, Eltarabily M.G. and Negm A.M, "Fundamentals of Groundwater Modeling Methods and a Focused Review on the Groundwater Models of the Nile Valley Aquifer," in Sustainability of Groundwater in the Nile Valley, Egypt, A. M. Negm and M. El-Rawy, Eds., Cham: Springer International Publishing, 2022, pp. 39–70. doi: 10.1007/978-3-031-12676-5_3.
- [15]Wang K. and Shih D.S, "A Method Combining Seepage Theory and Model Simulation for the Identification of Potential Groundwater Resources," Journal of Hydrologic Engineering, vol. 27, no. 12, p. 04022030, Dec. 2022, doi: 10.1061/(ASCE)HE.1943-5584.0002223.
- [16] Schwartz F.W. and Zhang H, Fundamentals of Groundwater. John Wiley & Sons, 2024.
- [17]Phoban H, Seeboonruang U, and Lueprasert P, "Numerical Investigation on Pile Behavior due to the Rising Groundwater Effect," GEOMATE Journal, vol. 20, no. 78, Art. no. 78, Nov. 2021.
- [18]Desitter A, Bates P.D, Anderson M.G. and Hervouet J.M, "Development of One, Two and Three-Dimensional Finite Element Groundwater Models within a Generalized Object-Oriented Framework," Hydrological Processes, vol. 14, no. 13, pp. 2245–2259, 2000, doi: 10.1002/1099-1085(200009)14:13<2245::AID-HYP26>3.0.CO;2-Q.
- [19]Idris Dag and Aynur Canivar, "Taylor-Galerkin Method for Advection-Diffusion Equation," Kybernetes, June 2011, doi: 10.1108/03684921111142304.
- [20]Karim I.A, Lee C.H, Gil A.J. and Bonet J, "A two-step Taylor-Galerkin Formulation for Fast Dynamics," Engineering Computations, vol. 31, no. 3, Art. no. 3, Apr. 2014, doi: 10.1108/EC-12-2012-0319.

- [21]Lewis R.W, Nithiarasu P. and Seetharamu K.N, Fundamentals of the Finite Element Method for Heat and Fluid Flow, 1st ed. Wiley, 2004. doi: 10.1002/0470014164.
- [22]Mehra M. and Kumar V, "Fast wavelet-Taylor Galerkin Method for Linear and Non-linear Wave Problems," Applied Mathematics and Computation, vol. 189, no. 2, pp. 1292–1299, June 2007, doi: 10.1016/j.amc.2006.12.013.
- [23]Roig B, "One-step Taylor-Galerkin Methods for Convection-Diffusion Problems," Journal of Computational and Applied Mathematics, vol. 204, no. 1, pp. 95–101, July 2007, doi: 10.1016/j.cam.2006.04.031.
- [24]Zienkiewicz O.C, Taylor R.L. and Nithiarasu P, The Finite Element Method for Fluid Dynamics, 6th edition. Amsterdam Heidelberg: Butterworth-Heinemann, 2005.

- [25]Nguyen T.H. and Thai H.P, "Assessment of Saltwater Intrusion into Bau Tro Lake when Fresh Water is Exploited in the Dry Season," in Proceedings of National Conference on Fluid Mechanics, Vietnam Publishing House of Natural Science and Technology, 2006, pp. 398– 415.
- [26]Kon Tum City Department of Science and Technology, "Scientific Report on the Implementation Results of the Kon Tum City Groundwater Project (1997–2000)," Department of Science and Technology, Kon Tum City, Viet Nam, 2001.

Copyright [©] Int. J. of GEOMATE All rights reserved, including making copies, unless permission is obtained from the copyright proprietors.